Egyptian Journal of Chemistry

Electrochemical Investigation of Terbinafine (C21H25N) as a Corrosion Inhibitor for Copper in a Molar Sulfuric Acid Solution

Said El Harrari *, Salim Ayoub , Driss Takky , Youssef Naimi
Laboratory of Physical Chemistry of Materials, Faculty of Sciences Ben M'sick, Hassan II University of Casablanca, Morocco

Abstract

In this work, a comprehensive study for using (2E)-N,6,6-triméthyl-N-(naphtalén-1-ylméthyl) hept-2-én-4-yn-1-amine as a corrosion inhibitor for copper in a Molar Sulfuric Acid Solution was performed. For this purpose, both types of electrochemical have been applied. The obtained experimental results showed that the investigated compound is a promising corrosion inhibitor for copper in acidic (0.5M H_2SO_4) environments. The inhibition efficiency increases with increasing inhibitor concentration. Adding a low inhibitor molecule(Terbinafine) concentration of about 5×10^{-3} M at 303K resulted in an inhibition efficiency of up to 95.20%. Terbinafine $C_{21}H_{25}N$ appears to have an anodic character, according to the polarization curves. Terbinafine protects the copper metal through adsorption on its surface by obstructing its active sites, according to Scanning electron microscopy SEM surface examination.

Keywords : Copper; Terbinafine; Corrosion inhibitor; Sulphuric acid;.. Electrochemical measurements; SEM surface.

1. Introduction

The growth of science and technology is intimately tied to the issues with corrosion and corrosion protection of metallic materials. [1]. Metallic materials' service life is impacted by corrosion caused by corrosive media when they are used [2]. Corrosion is the process by which the characteristics of metals generally deteriorate and disappear over time [3]. Metal corrosion not only results in some financial losses, but also worsens the working environment. Consequently, the study of metal corrosion protection has become a hot topic for experts in corrosion control [4]. One of the most affordable, practical, and useful techniques to prevent metal corrosion among them is the inclusion of a corrosion inhibitor [5].

The third largest non-ferrous metal produced globally, copper and its alloys are the oldest and most commonly utilized non-ferrous metals in human applications [6]. Because of its superior mechanical, thermal, and anti-fouling qualities as well as its good strength, flexibility, and wear resistance, it is crucial in many industrial applications [7, 8]. The majority of power plant condensers, low-pressure heating, and oil cooler heat exchangers, and water-cooled generator air conductors are all made of copper alloy materials.

Corrosion inhibitors are added to the acid wash solution to prevent the acid from corroding the copper itself, which is crucial because it also prevents the removal of the oxide coating from the copper surface [9]. Unfortunately, despite the fact that many corrosion-inhibiting materials possess outstanding corrosion-inhibiting properties, their applications are severely constrained by the significant risks they pose to both the environment and people [10]. Because of this, numerous corrosion protection experts have begun to explore and create new, highly effective, low-toxic, or even non-toxic corrosion inhibitors in recent years [11] [12]. Due to its low quantities, terbinafine can be taken orally and employed as a corrosion inhibitor. As a result, there is extremely little risk to both the environment and the human body. As is well known, heteroatoms like nitrogen, oxygen, sulfur, and other elements that have lone electron pairs typically make up corrosion inhibitor compounds [13], It successfully isolates the corrosive medium from the metal surface to protect it by forming coordination bonds with the vacant transition metal orbitals to create a thick protective coating. Terbinafine can be utilized as an inhibitor since it has a lot of heteroatoms and conjugated rings in it.

_____

*Corresponding author e-mail: Said.elharrari@gmail.com ; (Said El Harrari)

_____

2. Materials and Methods

Materials and Methods should be described with sufficient details to allow others to replicate and build on published results. Please note that the publication of your manuscript implies that you must make all materials, data, computer code, and protocols associated with the publication available to readers. Please disclose at the submission stage any restrictions on the availability of materials or information. New methods and protocols should be described in detail while well-established methods can be briefly described and appropriately cited.

Research manuscripts reporting large datasets that are deposited in a publicly available database should specify where the data have been deposited and provide the relevant accession numbers. If the accession numbers have not yet been obtained at the time of submission, please state that they will be provided during review. They must be provided before publication.

Interventional studies involving animals or humans, and other studies that require ethical approval must list the authority that provided approval and the corresponding ethical approval code.

3. The experimental part

3.1. Material and solution preparation

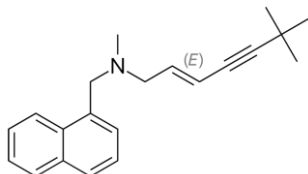We bought terbinafine from a neighborhood Moroccan pharmacy. In Fig.1, its molecular formula is displayed.

Fig. 1. Terbinafine ($C_{21}H_{25}N$) Structure.

Experiments were conducted using copper (in %) 99.98 and α-brass (60–40 copper–zinc) specimens. Utilizing concentrated, high-purity sulfuric acid and ultrapure water, the 0.5 M sulphuric acid corrosion solution was created. Terbinafine was then dissolved in the 0.5 M H_2SO_4 solution to provide the test solutions for 10^{-4}, 5.10^{-4}, 10^{-3}, and 5.10^{-3}, respectively.

The subsequent procedure is used to create the pure copper electrode. First, a linear cutter was used to cut the copper block into a 1 cm square. The next step was rough sanding using metallographic sandpaper with 180 grit. Only one side of the copper electrode was left exposed to the corrosive atmosphere after the remaining five sides were finally covered in a PVC (polyvinyl chloride) tube with epoxy.

3.2. Experiments with electrochemistry

The three-electrode setup was used for all electrochemical tests. In a 50 ml beaker, the entire three-electrode setup was put. The working electrode in this three-electrode setup is a 0.5 cm² pure copper electrode. The copper electrode was polished and flattened before each test using sandpaper with a mesh size of 400–2000. Platinum serves as the counter electrode. A linked saturated calomel electrode serves as the reference electrode.

The system is driven through an open circuit for around 40 minutes prior to the electrochemical testing. The signal has a frequency of 100,000 Hz, a low frequency of 0.01 Hz, an amplitude of 0.01 V, and a silent period of 2 s. Lastly, a test known as the potentiodynamic polarisation curve was conducted. The range of polarization ranged between E_{OCP} - 600 mV to E_{OCP} + 600 mV having a scan speed of 1 mV/s. To ensure that the results were accurate and repeatable, each experiment was run three times under identical circumstances.

3.3. Scanning Electron Microscopy of the surfaces

The necessary pure copper block was divided into three cubes, each with a side length of 0.3 cm before the copper slide was tested by SEM. Up till the test surface was level, the block was alternately sanded on 400-7000 mesh sandpaper. In the absence and presence of 5.10^{-3} M Terbinafine, two copper cubes were soaked independently in 0.5 M H_2SO_4 for 24 hours. The Hirox was used to analyze the samples.

4. Results and discussion

4.1. Curves of polarization

The potentiodynamic polarization curves of copper in 0.5M H_2SO_4 without and with Terbinafine at various concentrations are shown in Figure 2 in order to evaluate the corrosion inhibition process. By extrapolating from Tafel, one can derive certain significant characteristics, such as corrosion current density (I_{corr}), corrosion potential (E_{corr}), etc. The corrosion inhibition efficiency IE(in %) in equation (1) is determined from the corresponding corrosion current density, as indicated in the equation, and these polarization parameters are listed in Table (1) [14]:

$$IE_{(\%)} = ((I_{corr,0} - I_{corr}) / I_{corr,0}) \times 100 \quad (1)$$

Where $I_{corr,0}$, and I_{corr}, respectively, represent the corrosion current densities in the control solution and when Terbinafine is present.
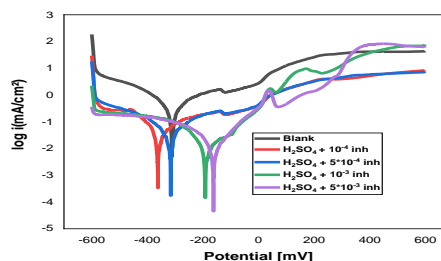

Fig. 2. Copper potentiodynamic polarization curves in a sulphuric acid solution without and with Terbinafine added
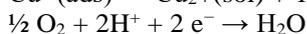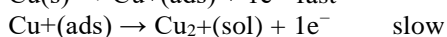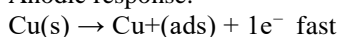
_____

Table 1 shows that the corrosion current density moves to lower values as Terbinafine concentrations rise. Without Terbinafine, the corrosion current density is 171.4 µA cm^{-2}. When the concentration of Terbinafine reaches 5.10^{-3} M, the corrosion current density rapidly decreases to 8.229 µA cm^{-2}. Additionally, Figure 2 makes it abundantly evident that at high Terbinafine concentrations, the slope of the polarization curves in the anodic zone dramatically increases. **[15]** This occurrence shows that the corrosion inhibitor molecules have desorbed from the copper electrode's surface. Furthermore, it is evident from Figure 2 that, following the addition of Terbinafine molecules, the cathodic polarisation curve's magnitude of the decline is noticeably bigger than that of the anode. This shows that the reduction of dissolved oxygen close to the electrode surface is successfully prevented by the addition of Terbinafine molecules. When the concentration of Terbinafine is increased, the corrosion potentials move from being negative for the first two concentrations to being positive for the last two concentrations, according to the trend of the fluctuation of corrosion potentials. If you look at Table 1, the shift towards the positive electrode is greater than 85 mV, which shows that the inhibitor is anodic in nature **[16]**.

**Table 1.** Terbinafine's polarization characteristics at various copper concentrations in 0.5 M H_2SO_4.

Concentrations of inhibitors (M)	E_{corr} (mV)	j_{corr} (µA/cm²)	b_a (mV/dec)	b_c (mV/dec)	IE (%)
---	-309	171.4	93.4	-83.9	---
10^{-4}	-361	36.99	172.9	-104.3	78.42
5.10^{-4}	-313	28.128	124.5	-120.2	83.59
10^{-3}	-189,9	9.3009	127.1	-82.7	94.57
5.10^{-3}	-162	8.229	100.5	-60.7	95.20

The following describes how copper corrodes in an acidic solution. The anode and cathode's response process is as follows. **[17]**:

Anodic response:

$Cu(s) \rightarrow Cu^+(ads) + 1e^-$ fast

$Cu^+(ads) \rightarrow Cu^{2+}(sol) + 1e^-$ slow

$\frac{1}{2} O_2 + 2H^+ + 2 e^- \rightarrow H_2O$

It is evident from the anode's corrosion mechanism that the copper substrate oxidizes quickly to cuprous ions. Consequently, many corrosion specialists think that copper's corrosion inhibition mechanism works as follows **[18]**:

$Cu^+ + $ *inhibitor molecule* $\rightarrow Cu^+$-*inhibitor molecule*
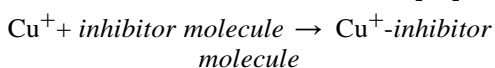
Because of this, the corrosion inhibitor molecule may more readily form a coordination bond with cuprous ions, effectively separating the corrosive medium from the copper substrate and resulting in a good corrosion prevention effect.

4.2. A test using electrochemical impedance spectroscopy

Terbinafine's inhibitory impact on copper at ambient temperature was investigated using the electrochemical impedance spectroscopy (EIS) experiment. Fig. 3 displays the Nyquist plots of copper in 0.5 M H_2SO_4 without and with various doses of Terbinafine.
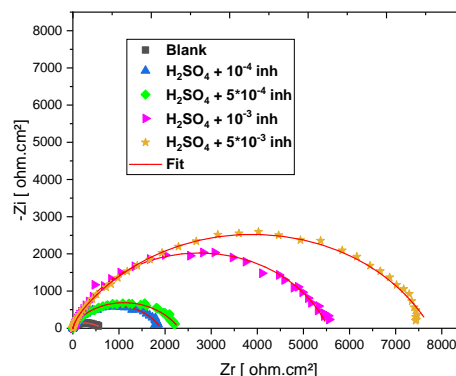

Fig. 3. Copper in sulfuric acid EIS plots in the absence and presence of various Terbinafine concentrations

The Warburg impedance is a straight line in the low frequency region of the Nyquist plots in the blank solution at various concentrations, as shown in Figure 3, while the capacitive reactance is an arc in the high frequency zone (typically related to the capacitance of the electrical double layer and the charge transfer resistance). The low frequency line indicates that with 0.5 M H_2SO_4, the copper has rusted. In other words, corrosion-related substances from the copper surface seep into the overall solution. The straight line in the low frequency zone vanishes as the terbinafine concentration rises, indicating that the copper surface corrosion product is effectively suppressed and diffusing into the bulk solution. Additionally, an increase in the charge transfer resistance of the copper electrode surface is to blame for the apparent growth in the radius of the capacitive reactance. These findings suggest that Terbinafine efficiently inhibits copper corrosion by creating a dense, resistant layer on the copper surface. Additionally, the uneven semicircles from which the capacitive reactance arc arises are connected to the heterogeneity of the copper surface **[19]**. The impedance measurements and the potentiodynamic polarisation experimental results are in good agreement.

The equivalent electrochemical impedance data were fitted using the two equivalent circuits, as illustrated in Figure 4. Table 2 contains the values of the fitted electrochemical parameters. R_f is the film resistance, whereas R_s is the solution resistance. R_{ct} implies that the corrosion reaction at the copper-solution contact is to blame for the charge transfer resistance. The Warburg impedance is W, CPE_f is the constant phase angle component made up of the deflection parameter n1

and the adsorbed inhibitor film capacitance C_f. CPE_{dl} It is made up of the deflection parameter n2 and an electrical double layer capacitor C_{dl}. The CPE impedance is represented by equation (2) as follows [20] :

$Z_{CPE} = 1/Y^0(jw)^n$ (2)

where j is the fictitious root and Y^0 is the admittance of the electrochemical system, ω displays the angular frequency, the deflection parameter is n. The values of C_f and C_{dl} are calculated with equation (3) by ω, n and Y^0 as follows [21]:

$C = Y^0(W)^{n-1} = Y^0(2\pi f_{z im-Max})^{n-1}$ (3)

where $f_{z im-Max}$ is the frequency corresponding to the maximum imaginary impedance.

Additionally, the equations for C_{dl} and C_f in the Helmholtz model are as follows. [22]:

$C_{dl} = ((\varepsilon^0 \varepsilon)/d)S$ (4)

$C_f = F^2 S/4RT$ (5)

where d is the distance between the metal surface and terbinafine. S is the surface area of copper exposed in the H_2SO_4 solution, ε^0 is the vacuum permittivity, ε is the local dielectric constant. F is the Faraday constant. The results of equations (4) and (5), it can be seen that the decrease in C_{dl} and C_f values is due to Terbinafine molecules replacing H_2O molecules on the copper surface. The equation used to compute the inhibition efficiency, the most crucial metric, is as follows :

$IE(\%) = ((R_{ct} - R_{ct},0)/R_{ct}) \times 100$ (6)

where R_{ct} and $R_{ct},0$ the charge transfer resistance
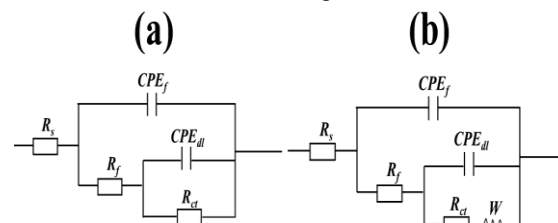
when Terbinafine is present and absent in H_2SO_4. Evidently, as Terbinafine concentration rises, corrosion inhibition effectiveness does as well. This is in line with the potentiodynamic polarization test results quite well.

Fig. 4. Equivalent circuits were utilized to fit the copper impedance spectra in sulfuric acid solution (b) and with terbinafine present (a)

Table 2. EIS parameters for the adjustment of Copper in 0.5 M H_2SO_4 at different temperatures with and without different concentrations of Terbinafine

| Inhibitor concentration, M	Rs (Ω cm^2)	Cf (F cm^{-2})	n1	Rf (Ω cm^2)	Cdl (F cm^{-2})	n2	Rct (Ω cm^2)	W (Ω−1 cm^{-2} s 0,5)	Rp=Rs + Rct (Ω cm^2)	IE(%)
---	1.192	0.52×10^{-3}	0.72	399.6	7.211×10^{-3}	0.53	221.4	0.38	621	---
10^{-4}	2.089	12.93×10^{-6}	0.95	13.57	84.11×10^{-6}	0.65	1900	---	1914	67..55
$5 \cdot 10^{-4}$	1.219	17.59×10^{-6}	0.94	1.65	120×10^{-6}	0.62	2304	---	2306	73.07
$10-3$	4.35	30.07×10^{-6}	0.92	895.6	45.88×10^{-6}	0.68	4650	---	5546	88.80
$5 \cdot 10^{-3}$	1.86	17.31×10^{-6}	0.89	1464	42.29×10^{-6}	0.66	6380	---	7772	92.01

4.3. SEM Surface Investigate

The features of the copper surfaces under various circumstances are shown in Figure 5. The characteristics of the copper surface after grinding are shown in Figure 5a. After soaking for 24 hours in 0.5 M H_2SO_4 with 5.10^{-3} Terbinafine, Figure 5b depicts the surface characteristic at 298.15 K. Without using any corrosion inhibitors, Figure 5c depicts the surface properties of copper submerged in 0.5 M H_2SO_4 at 298.15 K for 24 hours. As can be observed in Figure 5a, the polish left behind by the copper after SiC sandpaper grinding resulted in the naked copper showing noticeable nicks and lines after polishing. The pores left behind by the corrosion of copper in 0.5 M H_2SO_4 are plainly visible in Figure 5c. The copper surface is highly corroded, but these corrosion holes are remarkably uniform. The tight protective film barrier created by the Terbinafine investigated on the copper surface is depicted in Figure 5b. Additionally, the copper surface is remained smooth and homogene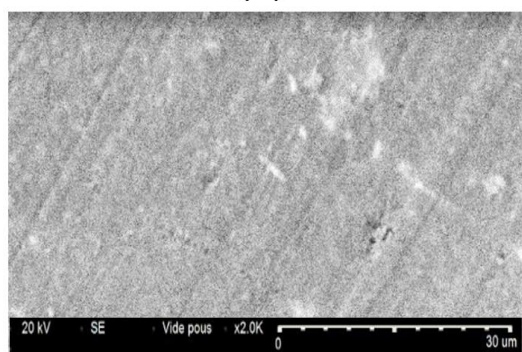ous 24 hours after being submerged in sulfuric acid. No noticeable corrosion holes are discovered, and some polishing-induced notches are still discernible. Since 5.10^{-3} Terbinafine can effectively block copper corrosion when added to the 0.5 M sulphuric acid solution, it can be shown by comparing the SEM patterns in Figure 5b and 5c.
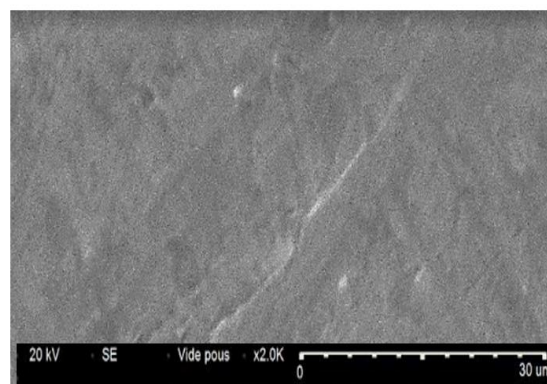
(a)
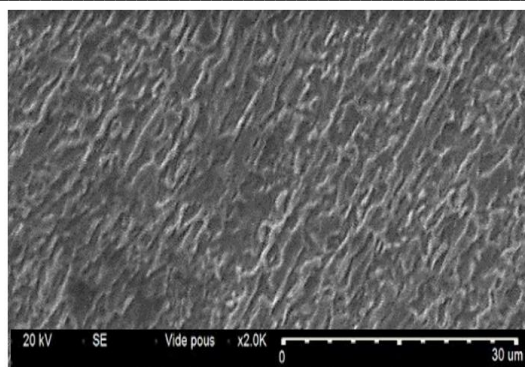
(b)

(c)

Fig. 5. Surface characteristics of copper in three different situations: (a) after grinding; (b) after 24 hours of soaking in 0.5 M H_2SO_4 at 298.15 K; and (c) after 24 hours of soaking in 0.5 M H_2SO_4 with the inhibitor.

5. Conclusions

Based on electrochemical tests, terbinafine inhibits anodic corrosion of copper in 0.5M/H_2SO_4. The electrochemical impedance spectroscopy under static conditions studies revealed that the best inhibition efficiency in optimum concentration (C=5.10^{-3}M (approx. 92%) at 298.15 .15 K are presented by the Terbinafine compound.

. Copper can be protected in sulfuric acid solution by the expired product Terbinafine. According to the data, the inhibition efficiency increases with the concentration of the inhibitor.

In order to effectively prevent copper corrosion, Terbinafine inhibitor molecule create a compact film on the copper surface, as shown in SEM photos. In addition, SEM analysis of copper coupons treated with sulfuric acid and terbinafine demonstrated the formation of a protective layer on the copper surface.

6. Conflicts of Interest

The authors declare that there is no conflict of interest regarding the publication of this paper

9. References

[1] Hanaa, M. E.; Omnia A. M.; Fouda, A. E. S. Artichoke Extract as an Eco-Friendly Corrosion Inhibitor for Zinc in 1 M Hydrochloric Acid Solution.Letters in Applied NanoBioScience, (2021), 10, 2655–2679

[2] Chugh, B.; Singh, A.K.; Thakur, S.; Pani, B.; Lgaz, H.; Chung, I.-M.; Jha, R.; Ebenso, E.E. Comparative Investigation of Corrosion-Mitigating Behavior of Thiadiazole-Derived Bis-Schiff Bases for Mild Steel in Acid Medium: Experimental, Theoretical, and Surface Study. ACS Omega (2020), 5, 13503-13520

[3] Benzbiria, N.; Echihi, S.; Belghiti, M.E.; Thoume, A.; Elmakssoudi, A.; Zarrouk, A.; Zertoubi, M.; Azzi, M. Novel synthetized benzodiazepine as efficient corrosion inhibitor for copper in 3.5% NaCl solution. Materials Today journal (2021) 37, 3932-3939

[4] Aralu, C.C.; Chukwuemeka-Okorie, H.O.; Akpomie, K.G. Inhibition and adsorption potentials of mild steel corrosion using methanol extract of Gongronema latifoliuim. Appl. Water Sci. (2021), 11, 1-7

[5] Sannaiah, P.N.; Alva, V.D.P.;Bangera, S. An experimental, theoretical, and spectral approach to evaluating the effect of eco-friendly Oxalis stricta leaf extract on the corrosion inhibition of mild steel in 1 N H2SO4 medium. J. Iran. Chem. Soc. (2022), 19, 1817-1835,

[6] Bangera, S.; Alva, V.D.; Pavithra, N.S. Averrhoa bilimbi leaf extract as a potent and sustainable inhibitor for mild steel in 1 M HCl medium: experimental and DFT enumeration. Chemistry Africa (2022) 5, 341-358,

[7] Echihi, S.; Benzbiria, N.; Belghiti, M.E.; El Fal, M.;
Boudalia, M.; Essassi, E.M.; Guenbour, A.; B ellaouchou, A.; Tabyaoui, M.; Azzi, M. Corrosion inhibition of copper by pyrazole pyrimidine derivative in synthetic seawater: Experimental and theoretical studies. Materials Today journal (2021) 37, 3958-3966

[8] Sodiya, E.F.; Dawodu, F.A. Leaf extracts as green substitute to toxic zinc chromate and zinc phosphate additives in Polyurethane primers for corrosion inhibition of steel. International

Review of Applied Sciences and Engineering (2021) 13, 80-87,

[9] Munawaroh, H. S. H.; Sunarya, Y.; Anwar, B.; et al. Protoporphyrin Extracted from Biomass Waste as Sustainable Corrosion Inhibitors of T22 Carbon Steel in Acidic Environments. Sustainability (2022) 14, 3622

[10] Eddy, N. O.; Odoemelam, S. A.; Ogoko, E. C.; et al. Experimental and Quantum Chemical Studies of Synergistic Enhancement of the Corrosion Inhibition Efficiency of Ethanol Extract of Carica Papaya Peel for Aluminum in Solution of HCl. Results in Chemistry (2022) 4, 100290

[11] Belghiti, M.E.; El Ouadi, Y.; Echihi, S.; Elmelouky, A.; Outada, H.; Karzazi, Y.; Bakasse, M.; Jama, C.; Bentiss , F.; Dafali, A. Anticorrosive properties of two 3,5-disubstituted-4-amino-1,2,4-triazole derivatives on copper in hydrochloric acid environment: Ac impedance, thermodynamic and computational investigations. Surfaces and Interfaces (2020) 21, 100692

[12] Deyab, M. A.; Mohsen, Q.; Guo, L. Aesculus Hippocastanum Seeds Extract as Eco-Friendly Corrosion Inhibitor for Desalination Plants: Experimental and Theoretical Studies. Journal of Molecular Liquids (2022) 361, 119594

[13] Hsissou, Rachid, et al. New epoxy composite polymers as a potential anticorrosive coatings for carbon steel in 3.5% NaCl solution: Experimental and computational approaches.Chemical Data Collections (2021) 31, 100619

[14] Hsissou, R; Abbout, S.; Benhiba, F.; Seghiri, R.; Safi, Z.; Kaya, S.; Briche, S.; Serdaroğlu, G.; Erramli, A.; Bachiri, E.; Zarrouk, A.; El Harfi, A. Insight into the corrosion inhibition of novel macromolecular epoxy resin as highly efficient inhibitor for carbon steel in acidic mediums: Synthesis, characterization, electrochemical techniques, AFM/UV– Visible and computational investigations, Journal of Molecular Liquids (2021) 337, 116492

[15] Belghiti, M.E.; Mihit, M.; Mahsoune, A.; Elmelouky, A.; Mghaiouini, R.; Barhoumi, A.; Dafali, A.; Bakasse, M.; El Mhammedi, M.A.; Abdennouri, M. Studies of Inhibition effect "E & Z'' Configurations of hydrazine Derivatives on Mild Steel Surface in phosphoiric acid. Journal of Materials Research and Technology (2019) 8, 6336-6353

[16] Ouakki, M.; Galai, M.; Benzekri, Z.; Verma, C.; Ech-chihbi, E.; Kaya, S.; Boukhris, S.; Ebenso, E.E.; EbnTouhami, M.; Cherkaoui, M. Insights into corrosion inhibition mechanism of mild steel in 1 M HCl solution by quinoxaline derivatives: electrochemical, SEM/EDAX, UV-visible, FT-IR and theoretical approaches. Colloids and Surfaces A: Physicochemical and Engineering Aspects (2021) 611, 125810

[17] El-Aal, A.; Sliem, M.; Abdullah, A. Caprylamidopropyl Betaine as a highly efficient eco-friendly corrosion inhibitor for API X120 steel in 1 M H2SO4. Egyptian Journal of Chemistry (2020) 63, 759-776

[18] Ali, E. H.; Himdan, T. A.; Ahmed, Z. W. Gallic Acid as Corrosion Inhibitor for Aluminum 6061 in Alkali Solutions. Ibn AL- Haitham Journal For Pure and Applied Sciences (2019) 32, 17–27

[19] Yadav, M.; Kumar, S.; Tiwari, N.; Bahadur, I.; Ebenso, E. E. Experimental and quantum chemical studies of synthesized triazine derivatives as an efficient corrosion inhibitor for N80 steel in acidic medium. J Mol Liq (2015) 212, 151–67

[20] Yadav, M.; Gope, L.; Kumari, N.; Yadav, P. Corrosion inhibition performance of pyranopyrazole derivatives for mild steel in HCl solution: Gravimetric, electrochemical and DFT studies. J. Mol. Liq (2016) 216, 78–86

[21] Roy, P.; Karfa, P.; Adhikari, U.; Sukul, D. Corrosion inhibition of mild steel in acidic medium by polyacrylamide grafted Guar gum with various grafting percentage: Effect of intramolecular synergism.Corros. Sci (2014) 88, 246-253

[22] Liu, Z.; Wang, D.; Li, D.; Wang, Hong-Q. The inhibition efficiencies of some organic corrosion inhibitors of iron: An insight from density functional theory study. Computational and theoretical chemistry (2022) 1214, 113759.